IMMUNODETECTION AND QUANTIFICATION OF ENZYMATIC MARKERS IN THECA CELLS: THE EARLY PROCESS OF OVARIAN STEROIDOGENESIS

P. Asiabi[1,*], E. C. R. Leonel[1, *], E. Marbaix[2, 3], M.M. Dolmans[1, 4], C.A. Amorim[1, **]

[1]Pôle de Recherche en Gynécologie, Institut de Recherche Expérimentale et Clinique, Université Catholique de Louvain, 1200 Brussels, Belgium

[2]Pathology Department, Cliniques Universitaires Saint-Luc, 1200 Brussels, Belgium

[3]Cell Biology Unit, de Duve Institute, Université Catholique de Louvain, 1200 Brussels, Belgium

[4]Gynecology and Andrology Department, Cliniques Universitaires Saint-Luc, 1200 Brussels, Belgium

* P. Asiabi and E.C.R. Leonel are joint first authors.

** Corresponding author:

Pôle de Recherche en Gynécologie

Institut de Recherche Expérimentale et Clinique

Université Catholique de Louvain

Avenue Mounier 52, bte B1.52.02, 1200 Brussels, Belgium

E-mail: christiani.amorim@uclouvain.be

Tel: +32 (0)2 764 5287

Downloaded from https://academic.oup.com/biolreprod/advance-article-abstract/doi/10.1093/biolre/ioz167/5554973 by Columbia University user on 02 September 2019

1. Abstract

The association between theca cells (TCs) and granulosa cells is pivotal to steroid biosynthesis in the ovary. During the late secondary follicle stage, TCs form a layer around granulosa cells, after which their steroidogenic function falls under the control of luteinizing hormone (LH) that activates the cAMP signaling pathway via a G protein-coupled receptor. In addition to perilipin-2, a marker for lipid droplets containing esters as substrates for TCs to produce steroidogenic hormones, other essential proteins, like steroidogenic acute regulatory protein (StAR), cytochrome P450 11A1, cytochrome P450c17, 3 beta-hydroxysteroid dehydrogenase/delta 5-->4-isomerase type 1, and 3 beta-hydroxysteroid dehydrogenase/delta 5-->4-isomerase type 2, play a role in the cascade after luteinizing hormone-choriogonadotropic hormone receptor (LH/CG-R) occupation by LH. The aim of the present study was to assess expression levels and corresponding amounts of LH/CG-R, perilipin-2 and enzymes involved in the steroidogenic pathway of TCs based on follicle stage. Immunohistochemical analysis of each of these proteins was therefore performed on ovarian samples from nine adult women, most (n=8) with BRCA1 and/or BRCA2 mutations undergoing prophylactic bilateral oophorectomy. Pictures were taken of the theca layer of secondary, small (<3000 µm) and large (>3000 µm) antral follicles and corpora lutea at 100X magnification. ImageJ software was used to analyze the surface area and expression intensity of each protein at each stage, known as the staining index. Overall, our data showed that LH/CG-R, perilipin-2 and StAR expression increased in the course of folliculogenesis and luteinization. Similarly, cytochrome P450 11A1, cytochrome P450c17, 3 beta-hydroxysteroid dehydrogenase/delta 5-->4-isomerase type 1, and 3 beta-hydroxysteroid dehydrogenase/delta 5-->4-isomerase type 2 expression were substantially elevated in TCs during folliculogenesis, evidenced by their coordinated action in terms of area covered and expression intensity. This study, conducted for the first time on human ovarian tissue, contributes to localizing and quantifying expression of key steroidogenic proteins at both intracellular and tissue levels. These findings may shed new light on pathological conditions involving the human ovary, such as androgen-secreting tumors of the ovary and other disorders associated with ovarian TCs in patients with polycystic ovary syndrome.

Downloaded from https://academic.oup.com/biolreprod/advance-article-abstract/doi/10.1093/biolre/ioz167/5554973 by Columbia University user on 02 September 2019

Key words: Enzyme / immunostaining / ovarian follicle / protein expression / steroid biosynthesis

Downloaded from https://academic.oup.com/biolreprod/advance-article-abstract/doi/10.1093/biolre/ioz167/5554973 by Columbia University user on 02 September 2019

2. Introduction

The ovary's ability to develop and release oocytes for fertilization is closely related to its endocrine activity (estradiol and progesterone synthesis), while a network between different cell types is required for follicles to grow and develop. This system includes mainly granulosa cells (GCs) and theca cells (TCs). GCs already surround oocytes by the time of birth [1], and originate from the mesonephros, which develops from the mesoderm layer during gastrulation [2]. TCs, on the other hand, are a group of differentiated cells that start to surround follicles only after their recruitment once they reach the secondary stage.

After follicle activation and initial growth, TCs and GCs act in a synergistic way, known as the two-cell, two-gonadotropin model, to initiate production of steroid hormones in response to luteinizing hormone (LH) and follicle-stimulating hormone (FSH) (reviewed by [3], [4]). Signaling pathways involved in steroid synthesis rely on cytoplasmic factors expressed by both types of cells; TCs convert cholesterol present in blood to androstenedione and testosterone, while GCs metabolize androstenedione to estradiol [1, 5]. TCs therefore perform a remarkable function in ovarian activity and play a crucial role in steroidogenesis in association with GCs, even in in vitro systems [6].

Steroid synthesis by follicular cells is based on proteins like steroidogenic acute regulatory protein (StAR), members of the cytochrome P450 family (11A1, c17 and aromatase) and 3 beta-hydroxysteroid dehydrogenase/delta 5-->4-isomerase types 1 and 2 (3-beta-HSD I and 3-beta-HSD II) [7]. Studies have reported expression of these proteins even before histological differentiation of the human fetal ovary occurs, as early as the 12th week of gestation [8], with levels of steroidogenic enzyme mRNA increasing in the second trimester of pregnancy [9]. Throughout this developmental phase, modifications in cytochrome P450 11A1, c17 and 3-beta-HSD II expression can already be seen [9]. However, actual steroid synthesis by TCs begins at puberty, when LH peaks become constant and receptor binding stimulates protein expression and androgen production [7]. TC steroidogenesis starts when the luteinizing hormone-choriogonadotropic hormone receptor (LH/CG-R) is occupied by LH, activating the cAMP signaling pathway via a G protein-coupled receptor. Cholesteryl esters stored in lipid droplets are substrates for androgen synthesis. Afterwards, cholesteryl esters stored in lipid droplets are translocated by StAR to the inner membrane of the mitochondria, where cytochrome

Downloaded from https://academic.oup.com/biolreprod/advance-article-abstract/doi/10.1093/biolre/ioz167/5554973 by Columbia University user on 02 September 2019

P450 11A1 converts it to pregnenolone, which is then converted to dehydroepiandrosterone (DHEA), androstenedione and progesterone in the presence of cytochrome P450c17, 3-beta-HSD I and 3-beta-HSD II in smooth endoplasmic reticulum.

The majority of available information on canonical mechanisms of follicle steroidogenesis relates to findings from species other than humans. However, it is important to bear in mind that interspecies differences are often reported [10] and human pathway patterns appear to be distinct in terms of tissue expression, activity and subcellular localization [11]. To the best of our knowledge, the specificity of the human steroidogenic pathway has not yet been documented in the ovary. Moreover, we do not know at which stage of follicle development different enzymes start to be expressed in human TCs. Apart from an obvious need to identify basic mechanisms of action, clarifying the workings of this cascade in human tissue would promote further advancement of TC differentiation experiments to support creation of new technologies, more specifically development of a bioengineered transplantable ovary.

The aim of this study was therefore to characterize human TCs at different stages of follicle development in relation to steroidogenic enzyme expression and quantification, lipid storage markers and LH/CG-R levels. Follicle growth stage was taken into account in order to ascertain temporal patterns and elucidate the sequence of their expression throughout folliculogenesis in the human ovary.

3. Materials and methods

3.1. Source of ovaries and ethical approval

Ovarian tissue samples used in this study were collected from nine adult women (age range: 35-43 years): eight patients were diagnosed with BRCA1 and/or BRCA2 mutations undergoing prophylactic bilateral salpingo-oophorectomy at Saint-Luc's University Hospital and one was bilaterally oophorectomized due to metastasis of pancreatic cancer to the left ovary (Supplementary Table 1). Each ovary was divided into fragments before fixation and dehydration, and embedded in several paraffin blocks (Supplementary Table 1). Analysis of the tissue samples by the anatomical pathology

Downloaded from https://academic.oup.com/biolreprod/advance-article-abstract/doi/10.1093/biolre/ioz167/5554973 by Columbia University user on 02 September 2019

department of the hospital did not reveal any modifications or anomalies in the ovaries used in our study. Each ovary contained follicles at different stages of development, as well as corpus luteum (CL). Use of human ovarian tissue was approved by the Institutional Review Board of the Université Catholique de Louvain on November 28, 2016 (IRB reference 2012/23MAR/125, registration number B403201213872).

3.2. Morphological evaluation and immunohistochemistry

Each paraffin block containing an ovarian tissue sample was serially sectioned (5-µm-thick sections) and every tenth slide was stained with hematoxylin and eosin (Merck, Darmstadt, Germany) for morphological analysis, follicle and CL localization, and measurement. The remaining slides (Superfrost® Plus, Menzel-Glaser, Braunschweig, Germany) were kept for immunostaining (Supplementary Table 1).

Immunohistochemical investigations were carried out using an indirect peroxidase method with a specific antibody for each of the seven selected proteins (Table 1). Briefly, after paraffin removal and rehydration, endogenous peroxidase activity was blocked by incubating the sections for 30 minutes in 3% H_2O_2. Antigen retrieval was performed in Tris EDTA buffer, pH 9.0, for 20 minutes at 96°C for LH/CG-R and cytochrome P450c17, or citrate buffer, pH 6.0, for 75 minutes at 98°C for the remaining antigens. Endogenous biotins were blocked only in the LH/CG-R protocol using an avidin-biotin kit (Vector, Burlingame, USA). Nonspecific binding was avoided by incubating sections in Tris-buffered saline with 5% bovine serum albumin (BSA) and 2% milk for LH/CG-R and cytochrome P450c17, or Tris-buffered saline with 10% normal goat serum (NGS) and 1% BSA for the rest. After incubation with primary antibody for 60 minutes for LH/CG-R and overnight for the other antibodies (see Table 1), the sections were incubated for a further 60 minutes at room temperature with secondary antibody: polyclonal goat anti-rabbit biotinylated immunoglobulin (Dako, USA) followed by streptavidin/horseradish peroxidase (HRP) for LH/CG-R, EnVision anti-mouse (Dako, USA) for perilipin-2 and 3-beta-HSD I, and EnVision anti-rabbit (Dako, USA) for StAR, cytochrome P450 11A1, cytochrome P450c17 and 3-beta-HSD II. The primary antibody was omitted in negative controls and a mixture of FLEX universal negative controls was added for rabbit or mouse antibodies

Downloaded from https://academic.oup.com/biolreprod/advance-article-abstract/doi/10.1093/biolre/ioz167/5554973 by Columbia University user on 02 September 2019

(Dako, USA). Sections were stained with a solution of diaminobenzidine (DAB) (Vector, Burlingame, USA) and counterstained with hematoxylin, before being dehydrated again and mounted for light microscopy analysis.

3.3. Follicle classification

Follicles were analyzed at different stages. Since the aim of this work was to elucidate and describe expression of steroidogenic proteins in TCs and luteal cells only, follicles at primordial and primary stages were not taken into account. Follicles were evaluated and classified as follows: secondary follicles with two or more cuboidal GC layers but no antrum; small antral follicles with an antrum but measuring less than 3 mm in diameter; and large antral follicles with an antrum and measuring more than 3 mm in diameter. Antral follicles with no GC layers or showing substantial apoptosis were excluded from the analysis. Regarding CL, no classification was made according to developmental stage.

3.4. Digitization and image analysis

The slides were analyzed by light microscopy (Nikon Eclipse, Tokyo, Japan) and digitized using a camera acquisition system (Leica DFC450, Leica Application Suite VA) at 100-fold magnification. The whole area of extension of secondary follicles was captured, so the total number of images taken of individual follicles at this stage ranged from 1 to 4, depending on their size. Antral follicles (small antral and preovulatory) required 6 images for adequate representation, with the exception of earlier stages of small antral follicles, which could be fully accommodated in fewer than 6 images. To ensure that the inner layers of the theca interna were investigated and in order to standardize the capture process for small antral and preovulatory follicles, one layer of GCs was included, delimiting the boundaries of the picture, as shown in Figure 1. This standardization also enabled TC layer localization and identification of the area to be studied. Concerning CL, 6 images were taken of the boundaries of the structures and evaluated in their entirety.

Analysis was undertaken using ImageJ software (version 1.52a, Wayne Rasband, NIH, USA). Irrespective of the number of images obtained, all underwent evaluation and mean values for each

Downloaded from https://academic.oup.com/biolreprod/advance-article-abstract/doi/10.1093/biolre/ioz167/5554973 by Columbia University user on 02 September 2019

were taken into consideration. Regions of interest (containing only TCs in case of follicles) were delineated manually. For CL, entire images were assessed, since small (paraluteal) and large luteal cells were intermingled. If present, folds, bubbles and artifacts were delimited and excluded prior to analysis by ImageJ. Color deconvolution was applied using hematoxylin and DAB vectors of the software to isolate DAB staining from tissue counterstaining. DAB staining was then detected using Rényi's entropy thresholding method (chosen according to stained versus non-stained tissue areas) and stained areas were measured. The same parameters were applied to all slides. Results were expressed for each follicle/CL as a staining index (SI) following the formula:

annotation proportion x percentage of stained area x staining intensity

where the annotation proportion is the percentage of delineated area in each picture of each individual follicle (n=1 to 6 images per follicle or CL), the percentage of stained area is calculated as (stained area/tissue area)*100, and staining intensity as (255 – mean intensity of stained pixels).

3.5. Statistical analysis

Statistical analysis was conducted using GraphPad Prism 5.0 software (GraphPad Software, Inc., CA, USA). For each immunohistochemical and antibody assay, the mean index obtained from all follicles in a given category was taken into account. Quantitative analysis was based on nonparametric (Kruskal-Wallis) evaluation of differences between the relevant developmental stages of follicles, followed by Dunn's multiple comparison tests. A p-value <0.05 was considered significant.

4. Results

The number of follicles and CL evaluated by category varied between patients and proteins, and is detailed in Table 2. Proteins were mostly present in TCs, but sometimes they were also expressed by other ovarian cells, such as GCs, oocytes or stromal cells. Expression patterns of each analyzed protein are described below and summarized in Tables 3 and 4 and Figures 5 and 6. Information on the stage of the menstrual cycle at the time of bilateral salpingo-oophorectomy was not recorded.

Downloaded from https://academic.oup.com/biolreprod/advance-article-abstract/doi/10.1093/biolre/ioz167/5554973 by Columbia University user on 02 September 2019

4.1 Expression patterns of different proteins in ovarian tissue

4.1.1 LH/CG-R

LH/CG-R was present in both cortical and medullary regions of the ovaries (Figure 2A and 2a). There were areas of focal staining in stromal cells (Figure 3C), where patterns of expression were usually cytoplasmic, but sometimes nuclear (Figure 3D). TCs showed intense immunostaining, making it easy to differentiate the TC layer from the surrounding stroma, even if some LH/CG-R-positive stromal cells were occasionally found. GCs and oocytes were negative for LH/CG-R. While CL exhibited widespread positive areas, staining intensity in these structures was not as strong as observed for other proteins. LH/CG-R expression in TCs was not significantly different between secondary, small and large antral follicles or CL ($p<0.2919$), but showed a tendency towards increasing patterns with follicle development and CL formation (Figure 5, LH/CG-R, and Figure 6A-1, A-2, A-3 and A-4).

4.1.2 Perilipin-2

Perilipin-2 was immunolabeled to investigate levels of lipid storage droplets in the cytoplasm of follicular cells at different developmental stages. This protein was only expressed in ovarian cortex, where weak staining was observed in bands of stromal cells. Some foci of darker perilipin-2 staining were identified in stroma surrounding follicle nests.

Despite some perilipin-2 expression in stromal fibroblasts, TC (from secondary follicles on) and luteal cell staining were much more intense than stromal staining (Figure 2B and b). In TCs, perilipin-2 expression was present in the cytoplasm (Figure 3H), limited to a thin theca interna layer (Figure 3G), but it was highly expressed throughout the whole cytoplasm of small circular luteal cells (Figure 6B-4). The cytoplasm of stromal cells was also perilipin-2-positive in areas surrounding CL. Perilipin-2 showed increasing expression patterns and was statistically significant in TCs of large antral follicles ($p<0.01$) and CL ($p<0.001$) versus secondary follicles, and in CL ($p<0.05$) versus small antral follicles (Figure 5, perilipin-2, and Figure 6B-1, B-2, B-3 and B-4).

4.1.3 StAR

Downloaded from https://academic.oup.com/biolreprod/advance-article-abstract/doi/10.1093/biolre/ioz167/5554973 by Columbia University user on 02 September 2019

Once cholesterol reaches the outer mitochondrial membrane, it is translocated to the inner membrane by StAR. StAR was immunolabeled in the cytoplasm of some TCs, but with no nuclear staining. Secondary and small antral follicles showed low levels of immunostaining for StAR (Figure 6C-1 and C-2 respectively), and large antral follicles (Figure 6C-3) somewhat minimal expression of this protein, limited to two or three inner layers of the theca interna (Figure 2c). It is important to point out that the TC layer was not consistently immunostained throughout the entire follicle (Figure 3K). GCs were StAR-negative, apart from those in the largest preovulatory follicle analyzed, which showed positive staining in their cytoplasm (Figure 3L). StAR expression was significantly elevated in TCs of small and large antral follicles ($p<0.001$) and CL ($p<0.01$) compared to TCs in secondary follicles (Figure 5, StAR, and Figure 6C-1, C-2, C-3 and C-4).

4.1.4 Cytochrome P450 11A1

Cytochrome P450 11A1 is located in the inner leaflet of the mitochondria and achieves the first step of steroidogenesis by converting cholesterol to pregnenolone. There were a few scattered foci of stromal cells in the cortex, showing enhanced cytoplasmic immunostaining for cytochrome P450 11A1 around the nucleus (Figure 4C). On the whole, no staining was observed in oocytes or GCs, and not all secondary follicles showed cytochrome P450 11A1-positive TCs. However, all TCs from small and large antral follicles were immunolabeled for cytochrome P450 11A1 (Figure 2D and 2d). In preovulatory follicles, only the cytoplasm of the inner theca interna layer was immunostained, but a few follicles also showed some expression in the cytoplasm and nucleus of GCs (Figure 4D). Cytochrome P450 11A1 expression was statistically higher in TCs of small ($p<0.001$) and large ($p<0.01$) antral follicles and CL ($p<0.001$) than in TCs of secondary follicles (Figure 5, cytochrome P450 11A1, and Figure 6D-1, D-2, D-3 and D-4).

4.1.5 Cytochrome P450c17

Cytochrome P450c17, and 3-beta-HSD I and 3-beta-HSD II are located in smooth endoplasmic reticulum and convert this steroid mainly to androstenedione in most species. When detected,

Downloaded from https://academic.oup.com/biolreprod/advance-article-abstract/doi/10.1093/biolre/ioz167/5554973 by Columbia University user on 02 September 2019

cytochrome P450c17 was specifically expressed in the cytoplasm of TCs (Figure 2E and e), starting as early as the secondary follicle stage (Figure 6E-1). The theca interna layer expressing this protein was very well delimited, but thin in some preovulatory follicles (Figure 4G). Since no immunolabeling was observed in other ovarian cells (Figure 2E and e), this marker can be considered specific to TCs and luteal cells. Often, cytochrome P450c17 was only expressed in the external layer of CL structures, where former TCs were present (Figure 4H), while central luteal cells, previously GCs, showed no immunostaining. Cytochrome P450c17 was not encountered at advanced CL stages, which were usually identified by cells with very small nuclei and a vacuolated cytoplasm, but exhibited increasing expression patterns in TCs of small ($p<0.05$) and large ($p<0.05$) antral follicles and CL (Figure 6E-1, E-2, E-3 and E-4), which were statistically significant.

4.1.6 3-beta-HSD I

Modest quantities of progesterone can be produced in TCs of growing follicles via conversion of pregnenolone by 3-beta-HSD I and 3-beta-HSD II. In CL, downregulation of cytochrome P450c17 allows pregnenolone to be converted to progesterone by these two isozymes, instead of DHEA. In this study, 3-beta-HSD I showed the strongest immunostaining among stromal cells, with numerous positive foci in extensive stromal areas of both the cortex and medulla (Figure 2F and f and Figure 4K). Very strong labeling was identified in the cytoplasm and nuclei of oocytes and GCs (Figure 6, F-1). TCs in secondary, small and large antral follicles also displayed 3-beta-HSD I immunostaining (Figure 6F-1, F-2 and F-3). Interestingly, preovulatory follicles exhibited a thin layer of TCs devoid of any immunolabeling, directly in contact with the basal lamina, while outer TC layers showed strong immunostaining in both the cytoplasm and nucleus of TCs (Figure 4L). Statistically significant expression patterns of 3-beta-HSD I were observed in TCs of secondary follicles versus small ($p<0.05$) and large ($p<0.05$) antral follicles and CL ($p<0.05$) (Figure 5, 3-beta-HSD I, and Figure 6F-1, F-2, F-3 and F-4).

4.1.7 3-beta-HSD II

Downloaded from https://academic.oup.com/biolreprod/advance-article-abstract/doi/10.1093/biolre/ioz167/5554973 by Columbia University user on 02 September 2019

In general, stromal cell staining was widespread, as with 3-beta-HSD I, and secondary follicles showed 3-beta-HSD II-immunostained TCs and GCs (Figure 4O and Figure 6G-1). No distinction was apparent between the extent of TC and stromal cell expression at this stage (Figure 6G-1). Small and large antral follicles both showed the presence of this protein in the cytoplasm and sometimes nuclei of TCs (Figure 6G-2 and G-3). Cytoplasmic staining was also constant in GCs in all follicles. In CL, immunolabeling appeared as small dots scattered throughout the cytoplasm (Figure 4P and Figure 6G-4). Expression of 3-beta-HSD II in TCs of follicles and CL showed a tendency to increase from the secondary to the small antral follicle stage, and was significantly higher in TCs of large antral follicles ($p<0.05$) than in TCs of secondary follicles (Figure 5, 3-beta-HSD II).

4.2 Quantification of protein expression: staining index

Means and standard errors of the SI calculated for each follicle stage and each protein are reported in Table 4. While all proteins showed increasing expression patterns during follicle development and CL formation, perilipin-2 (Figure 5, perilipin, and Figure 6B-1, B-2, B-3 and B-4), StAR (Figure 5, StAR, and Figure 6C-1, C-2, C-3 and C-4), cytochrome P450 11A1 (Figure 5, cytochrome P450 11A1, and Figure 6D-1, D-2, D-3 and D-4), cytochrome P450c17 (Figure 5, cytochrome P450c17, and Figure 6E-1, E-2, E-3 and E-4) and 3-beta-HSD II (Figure 5, 3-beta-HSD II, and Figure 6F-1, F-2, F-3 and F-4) exhibited significant increases in the SI from secondary follicles to the CL stage. On the other hand, the SI of LH/CG-R (Figure 5, LH/CG-R, and Figure 6A-1, A-2, A-3 and A-4) and 3-beta-HSD I (Figure 5, 3-beta-HSD I, and Figure 6G-1, G-2, G-3 and G-4) did not differ statistically between follicle stages or in CL.

5. Discussion

Looking to uncover new data on human TCs, we evaluated proteins related to steroidogenesis in follicles at different stages of development. While steroidogenic proteins are expressed in secondary follicles, they show different patterns of expression in growing follicles. Moreover, other ovarian

Downloaded from https://academic.oup.com/biolreprod/advance-article-abstract/doi/10.1093/biolre/ioz167/5554973 by Columbia University user on 02 September 2019

compartments also express most of these proteins, like cytochrome P450 11A1, 3-beta-HSD I and 3-beta-HSD II, but cytochrome P450c17 is the only protein expressed exclusively by TCs. While information on serum levels of sex steroids and menstrual cycle data may have aided interpretation of our results, taken together, these findings nevertheless add meaningful insights into the characterization of human ovarian tissue protein expression.

Steroidogenesis is coordinated by LH, and when it binds to its receptor LHR, TCs start intensifying their expression of steroidogenic protein-encoding genes [19, 20]. Previous studies have claimed that LH/CG-R localization is exclusively membranous [22], but the plasma membrane is internalized in coated vesicles, revealing cytoplasmic immunolabeling of this protein [23, 24], as evidenced in the present study already at the secondary stage **(**Figure 6A-1**)**. Takao et al. [24] also reported expression of LH/CG-R in secondary human follicles and small antral follicles. Its identification in preantral follicles suggests it may be a promoter of follicle development, as it is involved in the first steps of androgen biosynthesis. In CL, LH/CG-R staining decreases considerably across the luteal lifespan, becoming almost undetectable in regressing CL [24]. In the present study, it was not possible to determine CL age, but levels of LH/CG-R staining indicate that the majority of evaluated structures were in the infancy of their development.

Perilipin-2 is a lipid droplet-specific marker for identification of metabolically active cells [25]. Its functions in intracellular lipid droplet structuring and fatty acid transportation have already been described [26]. According to Talbott and Davis [27], LH regulates perilipin-2 phosphorylation via a cAMP signaling pathway, releasing the necessary substrate for steroidogenesis. Our results show abundant expression of perilipin-2 in CL (Figure 6B-4), which is consistent with CL function. Moreover, it correlates with Talbott and Davis's study [27] in bovine CL. These authors showed that bovine luteal tissue contains predominantly perilipin-2 and perilipin-3 lipid droplet coating proteins, as well as 3-beta-HSD I, cytochrome P450 11A1 and StAR [27].

StAR may confer acute [28] steroidogenic properties to previously non-steroidogenic cells and it is the first protein to play an actual role in cholesterol cleavage [29]. Its expression is mediated by protein kinases A and C and its regulation occurs in a tissue-, stimulus-, and species-specific manner [30]. Expression of StAR mRNA in human ovaries was previously reported only in TCs of preovulatory

Downloaded from https://academic.oup.com/biolreprod/advance-article-abstract/doi/10.1093/biolre/ioz167/5554973 by Columbia University user on 02 September 2019

follicles and luteal cells [31] by in situ hybridization [31]. However, this protein was sometimes found to be expressed in TCs of secondary and small antral follicles in the present study (Figure 6C-1 and C-2). It was also detected in GCs of some antral follicles. These follicles were nevertheless at very advanced stages, so it is possible that StAR expression was triggered by the start of the luteinization process, since GCs are not able to synthesize hormones directly from cholesterol [32]. Indeed, StAR is not expressed in GCs until the LH surge takes place [31]. Cytoplasmic immunohistochemical localization of StAR in the current study (Figure 6, C-1, -2, -3 and -4) could not determine exactly where in the mitochondria it resides, since such identification would require ultrastructural analysis. However, it is known that StAR promotes steroidogenesis only when present in the outer mitochondrial membrane, and loses its functionality when in the mitochondrial matrix [33].

Cytochrome P450 enzymes involved in steroidogenesis bind to the membranes of either mitochondria (11A1) or endoplasmic reticulum (c17) [11]. Cytochrome P450 11A1 is known to be a factor that promotes chronic steroidogenic activity and is implicated in the first cleavage step of biosynthesis [11] under the control of the cAMP signaling pathway [34]. Our findings in human ovarian tissue are inconsistent with results in rats, where cytochrome P450 11A1 was only found to be present at later follicle stages (Figure 6D-2 and -3) [35], but corroborate observations of peak expression levels in luteal cells (Figure 6D-4), as reported in cynomolgus moneys [36]. This suggests that in human CL, as in bovine CL [27], higher levels of cytochrome P450 11A1 are probably needed for progesterone synthesis.

Cytochrome P450c17 was localized in the perinuclear cytoplasm (Figure 6E-1, -2, -3 and -4), confirming its exclusive association with endoplasmic reticulum [37, 38]. It hydroxylates pregnenolone or progesterone and then cleaves C17-20 bonds to produce DHEA and androstenedione [11]. This protein was expressed in both TCs and paraluteal cells, but GCs do not express it [11] unless they are luteinized [39].

Both 3-beta-HSD I and 3-beta-HSD II are responsible for steroid reduction and oxidation. They are membrane-bound proteins distributed throughout the endoplasmic reticulum and in cristae of some TC mitochondria [11, 37], but their function and classification may be species-specific [40]. Indeed, 3-beta-HSD allows synthesis of steroid hormones. It was previously claimed that human 3-beta-HSD I

Downloaded from https://academic.oup.com/biolreprod/advance-article-abstract/doi/10.1093/biolre/ioz167/5554973 by Columbia University user on 02 September 2019

mRNA is only expressed in placenta, breast and skin [41], but this protein was identified throughout ovarian tissue in the present study (Figure 6F-1, -2, -3 and -4). Expression of 3-beta-HSD I and 3-beta-HSD II has also been reported in TCs and GCs of growing follicles in both human [42] (Figure 6F-1, -2, -3 and -4; G-1, -2, -3 and -4) and mouse [37] ovaries.

When assessing expression levels, a similar increase was encountered in StAR, cytochrome P450 11A1 and cytochrome P450c17 intensity during the process of folliculogenesis, but in luteinized cells, the SI was three times higher for cytochrome P450 11A1 than for StAR or cytochrome P450c17 (Figure 5). This was expected, since luteal cells are presumed to convert cholesterol directly to progesterone solely by the action of cytochrome P450 11A1 and 3-beta-HSD II [43]. However, the increase in 3-beta-HSD II expression was not as dramatic as that of cytochrome P450 11A1 when comparing CL and preovulatory follicles, which may be due to the fact that the 3-beta-HSD II SI was already high in preovulatory follicles.

Although follicles are self-sufficient structures in terms of steroidogenesis [44], it is not their exclusive role, as signs of steroidogenesis have also been reported in undifferentiated stromal cells [21], which could increase in pathological cases [45, 46]. Indeed, enzymes like 3-beta-HSD I and 3-beta-HSD II are widely expressed throughout the ovarian stroma, as demonstrated in our study (Figure 2F, f, G and g). While the ovaries used in our study appeared healthy, it is important to bear in mind that the patients were positive for BRCA1 and/or BRCA2 mutations and one of them had metastasis of pancreatic cancer. Northern blot and quantitative real-time polymerase chain reaction analyses have shown that cytochrome P450 11A1, cytochrome P450c17 and 3-beta-HSD II mRNA levels are higher in polycystic ovary syndrome (PCOS) cells than in their counterparts from healthy ovaries, while levels of StAR mRNA do not differ between PCOS cells and normal TCs [7], suggesting that StAR content does not vary significantly according to cell synthetic capacity.

In conclusion, each enzyme plays a specific and indispensable role in steroidogenesis, and silencing those genes that encode them diminishes steroid synthesis [47, 48]. As biosynthesis progresses along with follicle development, enzyme levels exhibit different expression patterns that have been detailed in the present work. On the whole, cytochrome P450 11A1, cytochrome P450c17 and 3-beta-HSD show substantially stronger expression in TCs during folliculogenesis, evidenced by both area covered

Downloaded from https://academic.oup.com/biolreprod/advance-article-abstract/doi/10.1093/biolre/ioz167/5554973 by Columbia University user on 02 September 2019

and immunostaining intensity. Other proteins that are important in steroid biosynthesis are LH/CG-R, perilipin-2 and StAR, whose expression also increases in the course of folliculogenesis and luteinization. Our findings are fundamental and may facilitate studies on pathological conditions affecting the human ovary, as well as the design and development of a bioengineered transplantable ovary.

6. Acknowledgments

The authors thank Mira Hryniuk for reviewing the English language of the manuscript, Dolores Gonzalez and Olivier Van Kerk for their technical assistance, and Dr. Caroline Bouzin (Imaging Platform from UCLouvain's Institute of Experimental and Clinical Research) for support with the analysis of data.

7. Authors' roles

P. Asiabi and E. C. R. Leonel: study design, experimental procedures, analysis, interpretation of data and manuscript preparation. E. Marbaix: tissue supply and manuscript preparation. M.M. Dolmans: manuscript preparation and revision. C. A. Amorim: experimental design, experimental procedures, interpretation of results and manuscript revision.

8. Funding

This study was supported by grants from the Fonds National de la Recherche Scientifique de Belgique [FNRS] (C. A. Amorim is an FRS-FNRS Research Associate; grant MIS #F4535 16 awarded to C. A. Amorim; grant 5/4/150/5 awarded to M. M. Dolmans; grant ASP-RE314 awarded to P. Asiabi) and the Fundação de Amparo à Pesquisa do Estado de São Paulo [FAPESP] (PhD grant 2016/22947-8 awarded to E. C. R. Leonel), and donations from the Ferrero family.

Downloaded from https://academic.oup.com/biolreprod/advance-article-abstract/doi/10.1093/biolre/ioz167/5554973 by Columbia University user on 02 September 2019

9. Conflict of interest

None of the authors has any competing interests to declare in relation to the topic.

10. References

1. Edson MA, Nagaraja AK, Matzuk MM. The Mammalian Ovary from Genesis to Revelation. Endocrine Reviews 2009; 30:624-712.
2. Kinder SJ, Tsang TE, Quinlan GA, Hadjantonakis AK, Nagy A, Tam PP. The orderly allocation of mesodermal cells to the extraembryonic structures and the anteroposterior axis during gastrulation of the mouse embryo. Development 1999; 126:4691-4701.
3. Hillier SG, Whitelaw PF, Smyth CD. Follicular oestrogen synthesis: the 'two-cell, two-gonadotrophin' model revisited. Molecular and Cellular Endocrinology 1994; 100:51-54.
4. Ryan KJ, Petro Z, Kaiser J. Steroid Formation by Isolated and Recombined Ovarian Granulosa and Thecal Cells. The Journal of Clinical Endocrinology & Metabolism 1968; 28:355-358.
5. Magoffin DA. Ovarian theca cell. The international journal of biochemistry & cell biology 2005; 37:1344-1349.
6. Honda A, Hirose M, Hara K, Matoba S, Inoue K, Miki H, Hiura H, Kanatsu-Shinohara M, Kanai Y, Kono T, Shinohara T, Ogura A. Isolation, characterization, and in vitro and in vivo differentiation of putative thecal stem cells. Proceedings of the National Academy of Sciences 2007; 104:12389-12394.
7. Wickenheisser JK, Nelson-DeGrave VL, McAllister JM. Human ovarian theca cells in culture. Trends in Endocrinology & Metabolism 2006; 17:65-71.
8. George FW, Wilson JD. Conversion of androgen to estrogen by the human fetal ovary. The Journal of Clinical Endocrinology & Metabolism 1978; 47:550-555.
9. Fowler PA, Anderson RA, Saunders PT, Kinnell H, Mason JI, Evans DB, Bhattacharya S, Flannigan S, Franks S, Monteiro A, O'Shaughnessy PJ. Development of Steroid Signaling Pathways during Primordial Follicle Formation in the Human Fetal Ovary. The Journal of Clinical Endocrinology & Metabolism 2011; 96:1754-1762.
10. Havelock JC, Rainey WE, Carr BR. Ovarian granulosa cell lines. Molecular and Cellular Endocrinology 2004; 228:67-78.
11. Payne AH, Hales DB. Overview of Steroidogenic Enzymes in the Pathway from Cholesterol to Active Steroid Hormones. Endocrine Reviews 2004; 25:947-970.
12. Kamada M, Yamano S, Irahara M, Aono T. Estrogen, progesterone--biosynthesis, receptor and action. Nihon rinsho. Japanese journal of clinical medicine 1997; 55:2865-2870.
13. Hu J, Zhang Z, Shen W-J, Azhar S. Cellular cholesterol delivery, intracellular processing and utilization for biosynthesis of steroid hormones. Nutrition & Metabolism 2010; 7:47-47.
14. Liu X, Cooper DE, Cluntun AA, Warmoes MO, Zhao S, Reid MA, Liu J, Lund PJ, Lopes M, Garcia BA. Acetate production from glucose and coupling to mitochondrial metabolism in mammals. Cell 2018; 175:502-513. e513.
15. Guo C, Shih M-C, Lan H-C, Hsu N-C, Hu M-C, Chung B-c. Transcriptional regulation of human CYP11A1 in gonads and adrenals. Journal of biomedical science 2007; 14:509-515.

Downloaded from https://academic.oup.com/biolreprod/advance-article-abstract/doi/10.1093/biolre/ioz167/5554973 by Columbia University user on 02 September 2019

16. Miller WL, Bose HS. Early steps in steroidogenesis: intracellular cholesterol trafficking: Thematic Review Series: Genetics of Human Lipid Diseases. Journal of Lipid Research 2011; 52:2111-2135.
17. Bose HS, Lingappa VR, Miller WL. Rapid regulation of steroidogenesis by mitochondrial protein import. Nature 2002; 417:87.
18. Bloom MS, Mok-Lin E, Fujimoto VY. Bisphenol A and ovarian steroidogenesis. Fertility and sterility 2016; 106:857-863.
19. McNatty KP, Makris A, Degrazia C, Rapin O, Ryan KJ. The Production of Progesterone, Androgens, and Estrogens by Granulosa Cells, Thecal Tissue, and Stromal Tissue from Human Ovaries in Vitro. The Journal of Clinical Endocrinology & Metabolism 1979; 49:687-699.
20. Zhang G, Garmey JC, Veldhuis JD. Interactive Stimulation by Luteinizing Hormone and Insulin of the Steroidogenic Acute Regulatory (StAR) Protein and 17α-Hydroxylase/17, 20-Lyase (CYP17) Genes in Porcine Theca Cells. Endocrinology 2000; 141:2735-2742.
21. McNATTY KP, MAKRIS A, DEGRAZIA C, RAPIN O, RYAN KJ. The production of progesterone, androgens, and estrogens by granulosa cells, thecal tissue, and stromal tissue from human ovaries in vitro. The Journal of Clinical Endocrinology & Metabolism 1979; 49:687-699.
22. Davis JS. Mechanisms of hormone action: luteinizing hormone receptors and second-messenger pathways. Current opinion in obstetrics & gynecology 1994; 6:254-261.
23. Ghinea N, Hai MV, Groyer-Picard M-T, Houllier A, Schoëvaërt D, Milgrom E. Pathways of internalization of the hCG/LH receptor: immunoelectron microscopic studies in Leydig cells and transfected L-cells. The Journal of Cell Biology 1992; 118:1347-1358.
24. Takao Y, Honda T, Ueda M, Hattori N, Yamada S, Maeda M, Fujiwara H, Mori T, Wimalasena J. Immunohistochemical localization of the LH/HCG receptor in human ovary: HCG enhances cell surface expression of LH/HCG receptor on luteinizing granulosa cells in vitro. Molecular human reproduction 1997; 3:569-578.
25. Straub BK, Gyoengyoesi B, Koenig M, Hashani M, Pawella LM, Herpel E, Mueller W, Macher-Goeppinger S, Heid H, Schirmacher P. Adipophilin/perilipin-2 as a lipid droplet-specific marker for metabolically active cells and diseases associated with metabolic dysregulation. Histopathology 2013; 62:617-631.
26. Gao J, Serrero G. Adipose differentiation related protein (ADRP) expressed in transfected COS-7 cells selectively stimulates long chain fatty acid uptake. Journal of Biological Chemistry 1999; 274:16825-16830.
27. Talbott H, Davis JS. Lipid Droplets and Metabolic Pathways Regulate Steroidogenesis in the Corpus Luteum. In: Meidan R (ed.) The Life Cycle of the Corpus Luteum. Cham: Springer International Publishing; 2017: 57-78.
28. Duarte A, Castillo AF, Podestá EJ, Poderoso C. Mitochondrial fusion and ERK activity regulate steroidogenic acute regulatory protein localization in mitochondria. PLoS One 2014; 9:e100387.
29. Lin D, Sugawara T, Strauss J, Clark B, Stocco D, Saenger P, Rogol A, Miller W. Role of steroidogenic acute regulatory protein in adrenal and gonadal steroidogenesis. Science 1995; 267:1828-1831.
30. Manna PR, Stetson CL, Slominski AT, Pruitt K. Role of the steroidogenic acute regulatory protein in health and disease. Endocrine 2016; 51:7-21.
31. Kiriakidou M, Mcallister JM, Sugawara T, Strauss 3rd J. Expression of steroidogenic acute regulatory protein (StAR) in the human ovary. The Journal of Clinical Endocrinology & Metabolism 1996; 81:4122-4128.
32. Hillier SG, Whitelaw PF, Smyth CD. Follicular oestrogen synthesis: the 'two-cell, two-gonadotrophin'model revisited. Molecular and cellular endocrinology 1994; 100:51-54.
33. Miller WL. Mechanism of StAR's regulation of mitochondrial cholesterol import. Molecular and Cellular Endocrinology 2007; 265-266:46-50.
34. Guo C, Hu M-C, Chung B-c. Transcriptional regulation of CYP11A1. Journal of biomedical science 2003; 10:593-598.

Downloaded from https://academic.oup.com/biolreprod/advance-article-abstract/doi/10.1093/biolre/ioz167/5554973 by Columbia University user on 02 September 2019

35. Oonk RB, Parker KL, Gibson JL, Richards JS. Rat cholesterol side-chain cleavage cytochrome P-450 (P-450scc) gene. Structure and regulation by cAMP in vitro. Journal of Biological Chemistry 1990; 265:22392-22401.
36. Ravindranath N, Little-Ihrig L, Benyo DF, Zeleznik AJ. Role of luteinizing hormone in the expression of cholesterol side-chain cleavage cytochrome P450 and 3 beta-hydroxysteroid dehydrogenase, delta 5-4 isomerase messenger ribonucleic acids in the primate corpus luteum. Endocrinology 1992; 131:2064-2070.
37. Pelletier G, Li S, Tremblay Y, Belanger A, Labrie F. Immunoelectron microscopic localization of three key steroidogenic enzymes (cytochrome P450 (scc), 3 beta-hydroxysteroid dehydrogenase and cytochrome P450 (c17)) in rat adrenal cortex and gonads. Journal of endocrinology 2001; 171:373-383.
38. Tamura T, Kitawaki J, Yamamoto T, Osawa Y, Kominami S, Takemori S, Okada H. Immunohistochemical localization of 17α-hydroxylase/C17–20 lyase and aromatase cytochrome P-450 in the human ovary during the menstrual cycle. Journal of Endocrinology 1992; 135:589-NP.
39. Morán FM, VandeVoort CA, Overstreet JW, Lasley BL, Conley AJ. Molecular Target of Endocrine Disruption in Human Luteinizing Granulosa Cells by 2,3,7,8-Tetrachlorodibenzo-p-Dioxin: Inhibition of Estradiol Secretion Due to Decreased 17α-Hydroxylase/17,20-Lyase Cytochrome P450 Expression. Endocrinology 2003; 144:467-473.
40. Abbaszade IG, Clarke TR, Park CH, Payne AH. The mouse 3 beta-hydroxysteroid dehydrogenase multigene family includes two functionally distinct groups of proteins. Molecular Endocrinology 1995; 9:1214-1222.
41. Eric R. Structure and expression of a new complementary DNA encoding the almost exclusive 3β-hydroxysteroid dehydrogenase/Δ5-Δ4-isomerase in human adrenals and gonads. Mol Endocrinol 1991; 5:1147-1157.
42. Breitenecker G, Friedrich F, Kemeter P. Further investigations on the maturation and degeneration of human ovarian follicles and their oocytes. Fertility and sterility 1978; 29:336-341.
43. Christenson LK, Devoto L. Cholesterol transport and steroidogenesis by the corpus luteum. Reproductive biology and endocrinology : RB&E 2003; 1:90-90.
44. Young JM, McNeilly AS. Theca: the forgotten cell of the ovarian follicle. Reproduction 2010; 140:489-504.
45. Blanco Jr LZ, Kuhn E, Morrison JC, Bahadirli-Talbott A, Smith-Sehdev A, Kurman RJ. Steroid hormone synthesis by the ovarian stroma surrounding epithelial ovarian tumors: a potential mechanism in ovarian tumorigenesis. Modern Pathology 2017; 30:563.
46. Nagamani M, Urban RJ. Increased expression of messenger ribonucleic acid encoding cytochrome P450 cholesterol side-chain cleavage and P450 17α-hydroxylase enzymes in ovarian hyperthecosis. Fertility and Sterility 1999; 71:328-333.
47. Li Y, Liang X-y, Wei L-n, Xiong Y-l, Yang X, Shi H-g, Yang Z-h. Study of RNA interference inhibiting rat ovarian androgen biosynthesis by depressing 17alpha-hydroxylase/17, 20-lyase activity in vivo. Reproductive Biology and Endocrinology 2009; 7:73.
48. Huang C-CJ, Shih M-CM, Hsu N-C, Chien Y, Chung B-c. Fetal Glucocorticoid Synthesis Is Required for Development of Fetal Adrenal Medulla and Hypothalamus Feedback Suppression. Endocrinology 2012; 153:4749-4756.

Figure and table legends

Figure 1. Photomicrograph showing the protocol used to analyze images. Each picture of small and large antral follicles was taken in such a way that one layer of GCs could be identified (shown here by

Downloaded from https://academic.oup.com/biolreprod/advance-article-abstract/doi/10.1093/biolre/ioz167/5554973 by Columbia University user on 02 September 2019

a dashed red line). The area containing only TCs was then selected by the software tool for quantification analysis (A). After selection of the area of interest, deconvolution was applied and the DAB-stained area and its intensity were quantified (B). Bar: 20 µm. GC: granulosa cell; TC: theca cell.

Figure 2. Lower magnification photomicrographs of human ovary immunostained with LH/CG-R (A and a), perilipin-2 (B and b), StAR (C and c), cytochrome P450 11A1 (D and d), cytochrome P450c17 (E and e), 3-beta-HSD I (F and f) and 3-beta-HSD II (G and g). Capital letters represent 4X magnified photomicrographs (bar: 500 µm) and small letters 10X magnified images (bar: 200 µm).

Figure 3. Photomicrographs of controls highlighting immunohistochemical patterns of LH/CG-R, perilipin-2 and StAR in ovarian tissue. Negative and positive controls for each protein respectively: adrenal gland (A and B), liver (E and F) and testes (I and J). LH/CG-R showed focal staining on the cortex (C), with cytoplasmic and nuclear staining in fibroblasts (D). Perilipin-2 was present in a thin theca interna layer (G) as faint dots in the cytoplasm (H). Some small antral follicles displayed focal expression of StAR in the theca layer (K), and a few preovulatory follicles showed some immunolabeling in GCs (L). Bars: 20 µm in H; 50 µm in G and D; 100 µm in A, B, E, F, I, J and K; and 200 µm in C. GC: granulosa cell; TI: theca interna; TE: theca externa.

Figure 4. Photomicrographs of controls highlighting immunohistochemical patterns of cytochrome P450 11A1, cytochrome P450c17, 3-beta-HSD I and 3-beta-HSD II in ovarian tissue. Negative and positive controls for each protein respectively: testes (A and B), adrenal gland (E and F) and placenta (I, J, M and N). Cytochrome P450 11A1 showed strong perinuclear cytoplasmic staining (C), while GC staining was present only in some preovulatory follicles (D). The theca interna layer expressing cytochrome P450c17 was very well delimited (G), and considerably stronger staining was detected in the outer CL layer, suggesting the presence of paraluteal cells (H). 3-beta-HSD I was the protein showing the highest expression throughout stromal cells (K). GCs and oocytes were also 3-beta-HSD I-immunostained, while preovulatory follicles exhibited a thin layer of TCs unstained for 3-beta-HSD

Downloaded from https://academic.oup.com/biolreprod/advance-article-abstract/doi/10.1093/biolre/ioz167/5554973 by Columbia University user on 02 September 2019

I (*) directly between the basal lamina and the immunolabeled theca interna layer (L). A secondary follicle can be seen with 3-beta-HSD II immunostaining in GCs and the oocyte (O), with patterns of luteal cell expression visible in the cytoplasm (P). Bars: 20 µm in C, D and P; 50 µm in G and O; 100 µm in A, B, E, F, H, I, J, L, M and N; and 200 µm in K. GC: granulosa cell; CL: corpus luteum; TC: theca cell.

Figure 5. Immunostaining quantification of different proteins at each follicle stage expressed as mean ± standard error. Each graph corresponds to every enzyme involved in TC steroidogenesis. The Y axis represents the SI and the X axis represents different stages of follicle development and CL. Lines between follicle stages and CL indicate statistically significant differences according to both the Kruskal-Wallis test and Dunn's multiple comparison test. Values are divided by 1000. TC: theca cell; SI: staining index; CL: corpus luteum.

Figure 6. Representative images of secondary, small and large antral follicles and CL. Note the differences between the intensity and area of each protein: LH/CG-R (A), perilipin-2 (B), StAR (C), cytochrome P450 11A1 (D), cytochrome P450c17 (E), 3-beta-HSD I (F) and 3-beta-HSD II (G). Secondary (1), small antral (2), and large antral (3) follicles and CL (4). Measurement bars: 20 µm. CL: corpus luteum.

Table 1. Antibodies and immunohistochemical protocols applied.

Table 2. Total number of follicles and CL analyzed for each protein.

Table 3. Expression of proteins in different ovarian tissue compartments.

Table 4. Means ± standard error of the SI of each protein of interest calculated for each follicle stage, including CL.

Downloaded from https://academic.oup.com/biolreprod/advance-article-abstract/doi/10.1093/biolre/ioz167/5554973 by Columbia University user on 02 September 2019

Supplementary Table 1. Ovarian tissue used in this study.

Downloaded from https://academic.oup.com/biolreprod/advance-article-abstract/doi/10.1093/biolre/ioz167/5554973 by Columbia University user on 02 September 2019

Fig-1

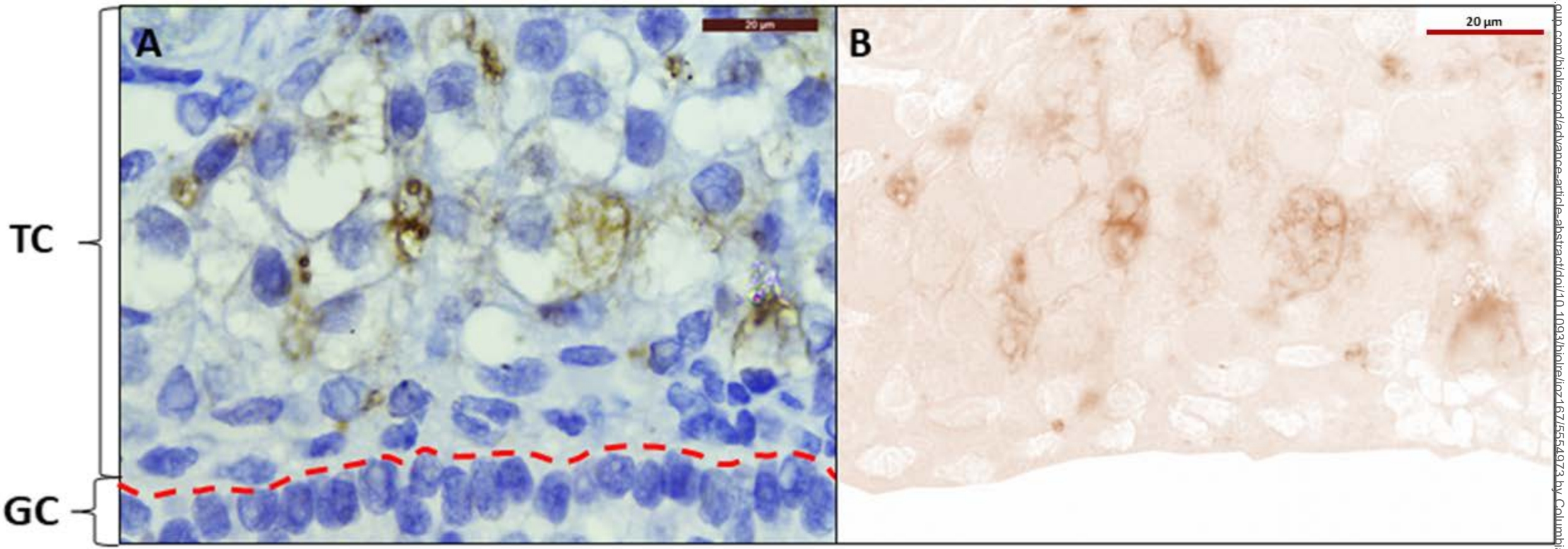

Downloaded from https://academic.oup.com/biolreprod/advance-article-abstract/doi/10.1093/biolre/ioz167/5554973 by Columbia University user on 02 Septembe

Fig-2

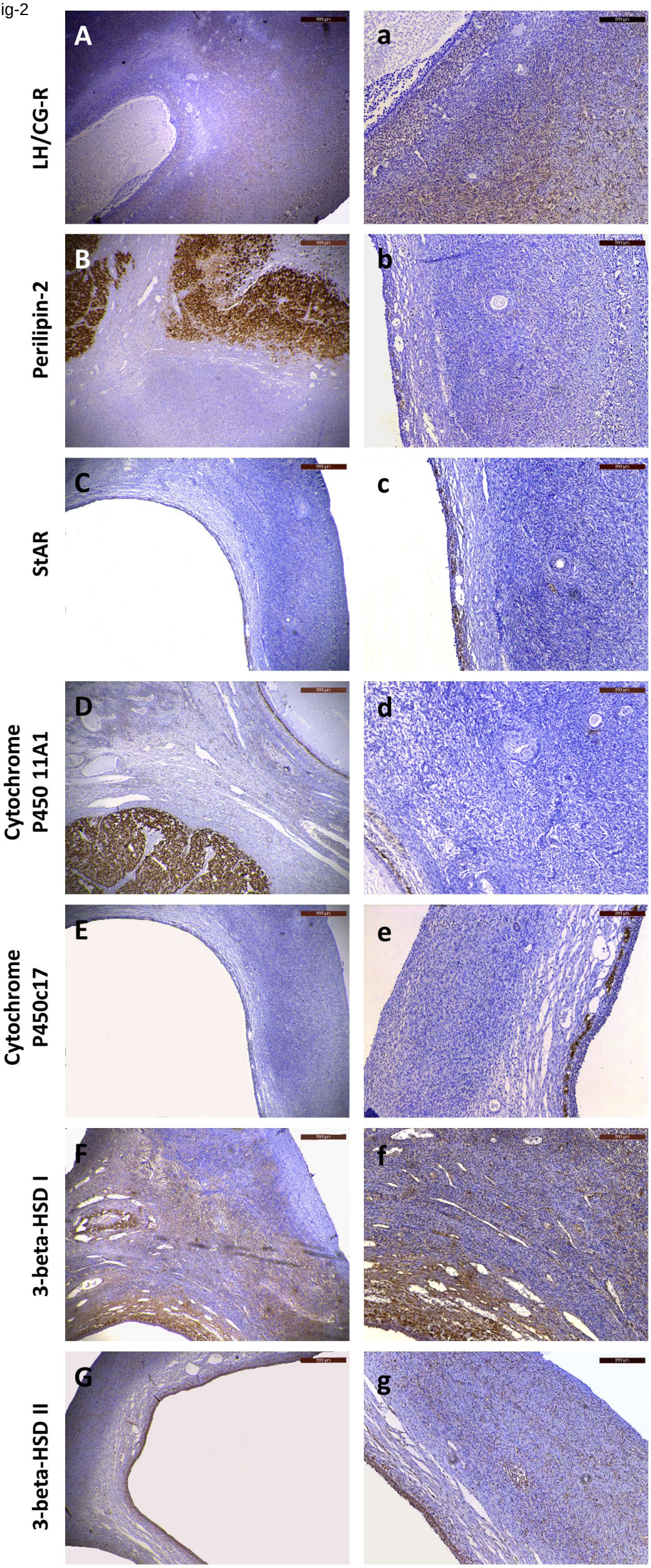

Downloaded from https://academic.oup.com/biolreprod/advance-article-abstract/doi/10.1093/biolre/ioz167/5554973 by Columbia University user on 02 September 2019

Fig-3

aded from https://academic.oup.com/biolreprod/advance-article-abstract/doi/10.1093/biolre/ioz167/5554973 by Columbia University user on 02 Septemb

Fig-4

aded from https://academic.oup.com/biolreprod/advance-article-abstract/doi/10.1093/biolre/ioz167/5554973 by Columbia University user on 02 Septembe

Fig-5

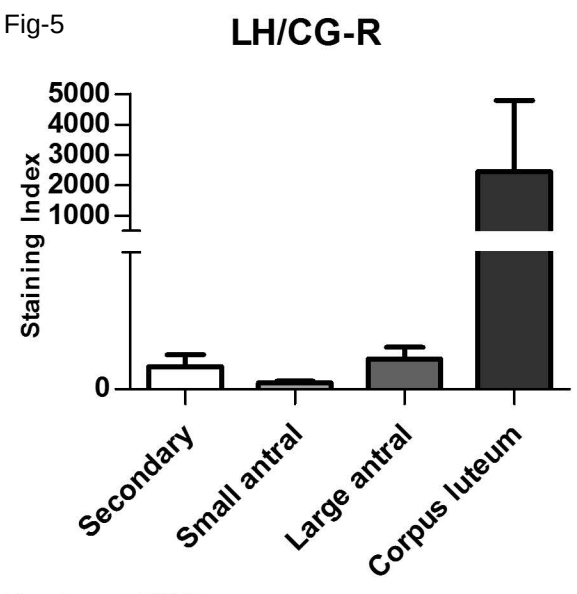

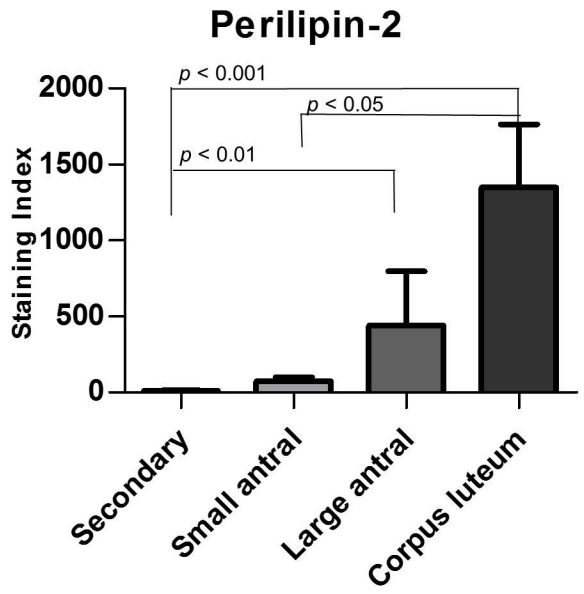

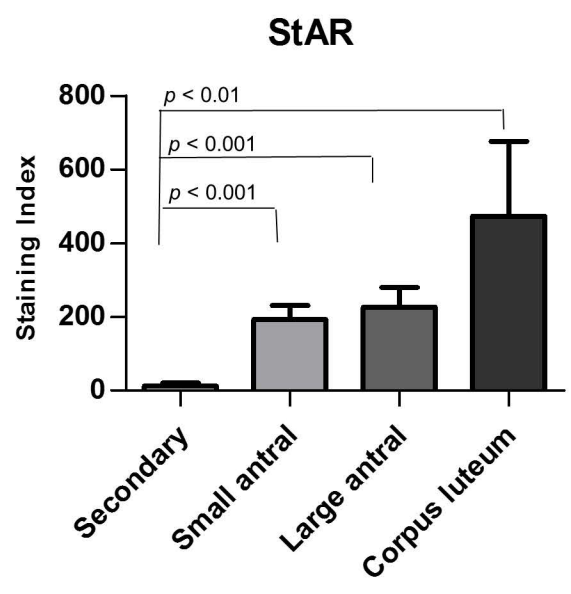

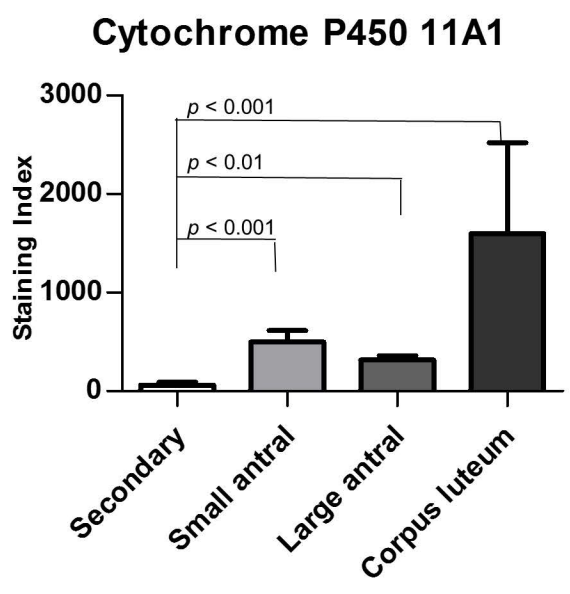

P value = 0,2919

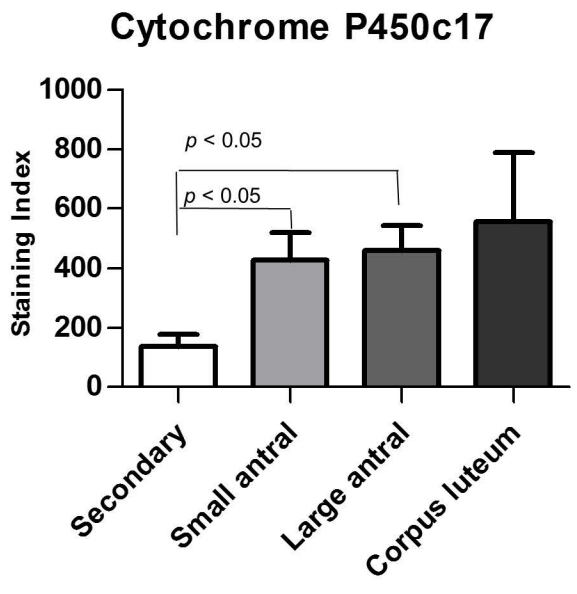

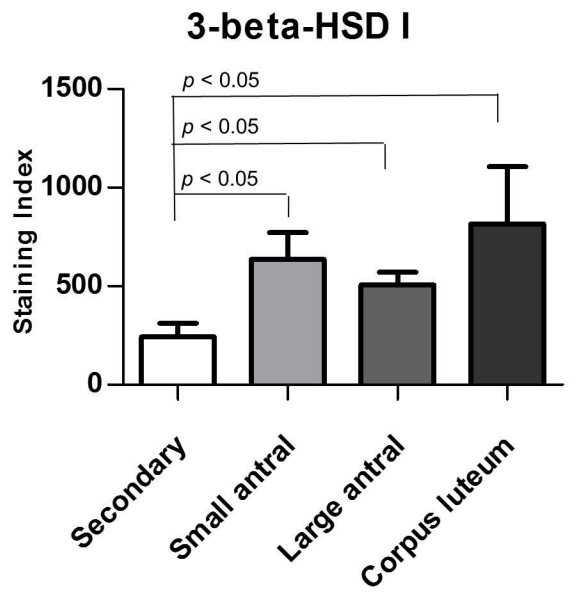

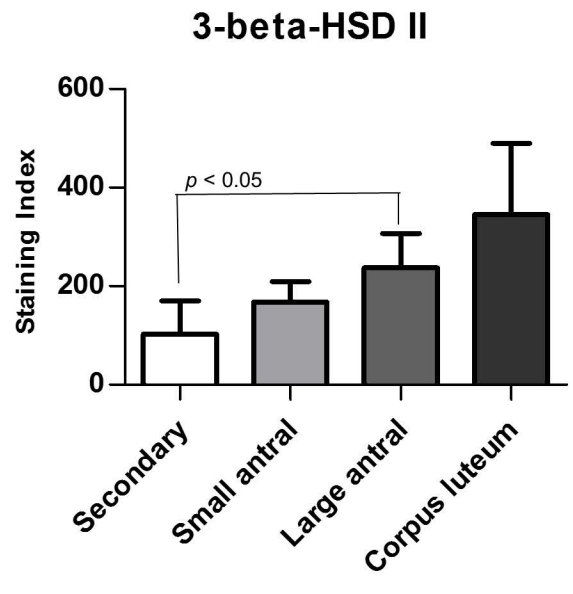

Downloaded from https://academic.oup.com/biolreprod/advance-article-abstract/doi/10.1093/biolre/ioz167/5554973 by Columbia University user on 02 Septembe

Fig-6

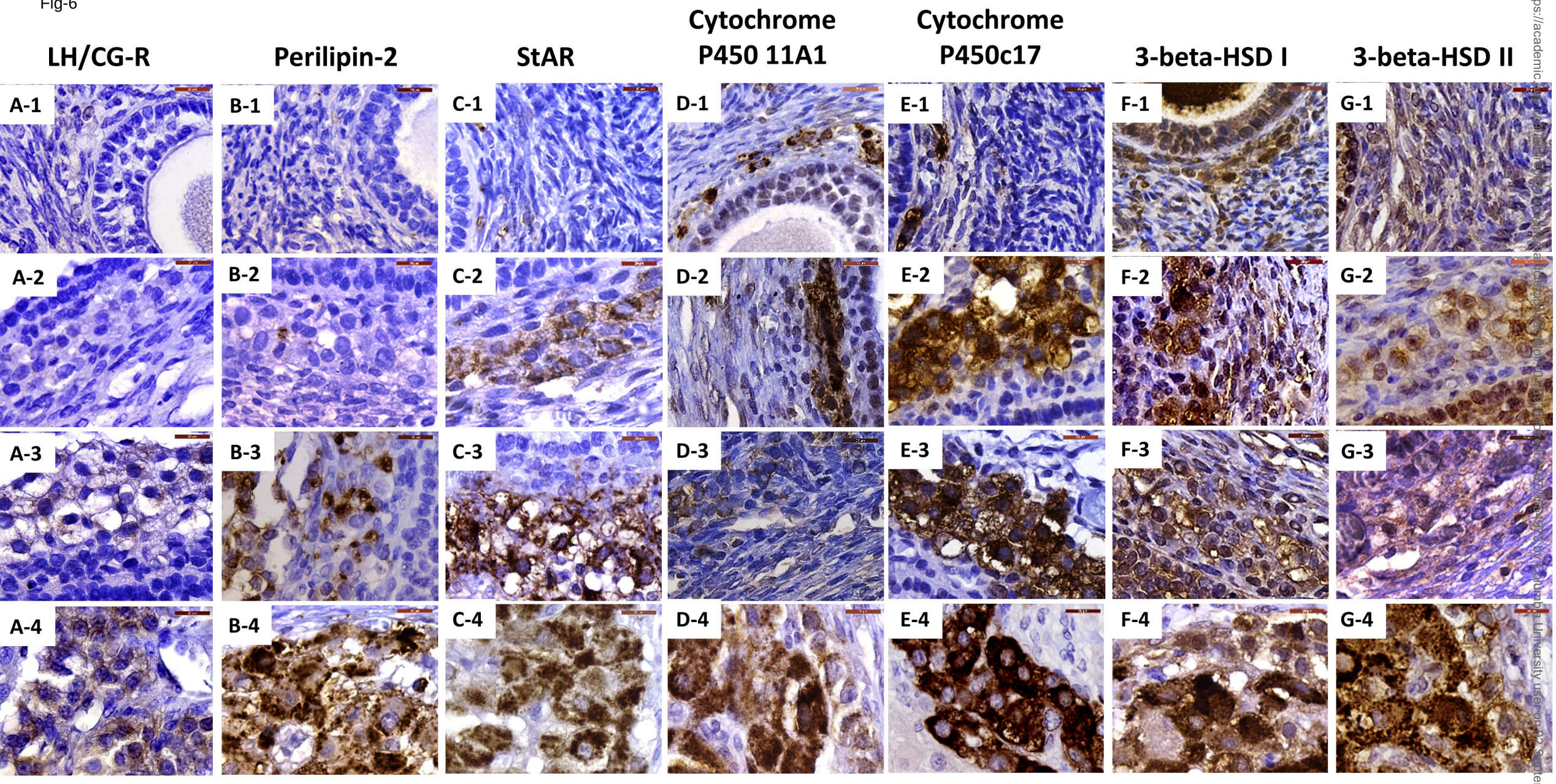

Downloaded from https://academic.oup.com/humrep/article-abstract/10/10/2674/640373 by Columbia University user on 02 September

Table 1. Antibodies and immunohistochemical protocols applied.

Antigen	Antibody type	Dilution	Incubation	Positive control
LH/CG-R (PA5-21271; ThermoFisher Scientific, Rockford, USA)	Polyclonal (rabbit)	1:1000 in TBS + 5% BSA + 2% milk	RT 1h	Adrenal gland
Perilipin-2 (SC-377429; Santa Cruz Biotechnology, Santa Cruz, USA)	Monoclonal (mouse)	1:200 in TBS + 1% NGS + 0.1% BSA	4°C O/N	Liver
StAR (AB133657; Abcam, Cambridge, UK)	Monoclonal (rabbit)	1:200 in TBS + 1% NGS + 0.1% BSA	4°C O/N	Testes and placenta
Cytochrome P450 11A1 (HPA016436; Sigma Aldrich/Merck, Darmstadt, Germany)	Polyclonal (rabbit)	1:1000 in TBS + 10% NGS + 1% BSA	4°C O/N	Testes
Cytochrome P450c17 (ORB5948; Biorbyt, Cambridge, UK)	Polyclonal (rabbit)	1:200 in TBS + 2.5% BSA + 1% milk	4°C O/N	Adrenal gland
3-beta-HSD I (AB55268; Abcam, Cambridge, UK)	Monoclonal (mouse)	1:100 in TBS + 1% NGS + 0.1% BSA	4°C O/N	Placenta
3-beta-HSD II (GTX102813; Genetex, San Antonio, USA)	Polyclonal (rabbit)	1:500 in TBS + 1% NGS + 0.1% BSA	4°C O/N	Placenta

TBS: tris-buffered saline; BSA: bovine serum albumin; RT: room temperature; NGS: normal goat serum; O/N: overnight

Downloaded from https://academic.oup.com/biolreprod/advance-article-abstract/doi/10.1093/biolre/ioz167/5554973 by Columbia University user on 02 September 2019

Table 2. Total number of follicles and corpora lutea analyzed for each protein.

Follicle category	Proteins						
	LH/CG-R	Perilipin-2	StAR	Cytochrome P450 11A1	Cytochrome P450c17	3-beta-HSD I	3-beta-HSD II
Secondary	12	13	18	17	12	15	10
Small antral	11	11	10	10	11	10	7
Preovulatory	19	16	17	15	17	14	14
Corpus luteum	7	7	5	5	4	4	7
Total	49	47	50	47	44	43	38

Downloaded from https://academic.oup.com/biolreprod/advance-article-abstract/doi/10.1093/biolre/ioz167/5554973 by Columbia University user on 02 September 2019

Table 3. Expression of proteins in cells from different ovarian tissue compartments.

	From follicle compartments						From ovarian stroma	
	TC from different stages of follicle development				GC	Oocyte	Cortex	Medulla
	Secondary	Small antral	Large antral	CL				
LH/CG-R	+	+	+	+	-	-	+	+
Perilipin-2	+/-	+	+	+	-	-	-	+
StAR	+/-	+/-	+	+	+	+	-	-
Cytochrome P450 11A1	+/-	+	+	+	+	-	-	+
Cytochrome P450c17	+	+	+	+	-	-	-	-
3-beta-HSD I	+	+	+	+	+	+	+	+
3-beta-HSD II	+	+	+	+	+	+	+	+

(-) no structure analyzed showed immunostained cell; (+/-)some structures with and some without immunostained cells; (+) all structures showed immunostained cells.

Downloaded from https://academic.oup.com/biolreprod/advance-article-abstract/doi/10.1093/biolre/ioz167/5554973 by Columbia University user on 02 September 2019

Table 4. Mean ± standard error of the SI of each protein of interest calculated for each follicle stage, including corpus luteum.

Protein	Secondary	Small antral	Preovulatory	Corpus luteum
LH/CG-R	83.25 ± 42.85[a]	23.02 ± 6.20[a]	110.57 ± 43.14[a]	2441.49 ± 2351.74[a]
Perilipin-2	9.15 ± 4.41[a]	72.86 ± 29.00[a,b]	438.74 ± 359.22[b,c]	1349.71 ± 413.70[c]
StAR	12.57 ± 8.24[a]	192.48 ± 38.10[b]	225.96 ± 54.45[b]	473.62 ± 203.02[b]
Cytochrome P450 11A1	59.54 ± 30.55[a]	499.80 ± 114.89[b]	313.17 ± 44.56[b]	1594.20 ± 924.01[b]
Cytochrome P450c17	136.42 ± 41.17[a]	426.24± 94.32[b]	460.31 ± 82.37[b]	556.42 ± 233.23[a,b]
3-beta-HSD I	241.81 ± 69.24[a]	634.95 ± 136.15[a]	505.69 ± 64.90[a]	816.63 ± 288.82[a]
3-beta-HSD II	102.38 ± 68.05[a]	167.08 ± 42.02[a,b]	236.97 ± 70.13[b,c]	344.79 ± 144.50[c]

Different superscript letters in the same row represent significant differences (p<0.05) between the follicle categories. Values are divided by 1000.

Downloaded from https://academic.oup.com/biolreprod/advance-article-abstract/doi/10.1093/biolre/ioz167/5554973 by Columbia University user on 02 September 2019